# 10

# The pinch technique for electroweak theory

In this chapter, we give a general overview of how the pinch technique (PT) is modified in the case of a theory with spontaneous (tree level) symmetry breaking (Higgs mechanism) [1, 2, 3], using the electroweak sector of the standard model as the reference theory.

The application of the pinch technique in the electroweak sector brings about significant conceptual and practical advantages. First, from the purely theoretical point of view, it is important to know that the PT construction is sufficiently general to encompass theories other than massless Yang–Mills. Though the required technical manipulations in the electroweak sector turn out to be fairly cumbersome, the basic underlying principles are practically the same; what increases the complexity is not the principle itself but rather the proliferation of fields and vertices involved. In addition, the PT algorithm exposes systematically the vast number of cancellations that take place when the (nonrenormalizable) Green's functions of the unitary gauge are put together to form physical amplitudes. In fact, one may start directly from the unitary gauge and derive the same PT Green's function constructed in the context of the (renormalizable) $R_\xi$ gauges. The application of the pinch technique provides a deeper understanding of the connection between the unitary gauge and the optical theorem and analyticity. Moreover, in the context of a theory with symmetry breaking, one gains new, important insights on the connection between the pinch technique and the background field method (BFM). Specifically, the BFM Feynman gauge is uniquely and unambiguously singled out by the powerful physical requirement of having Green's functions that display only *physical thresholds*. Last, but not least, one may derive crucial Ward identities, relating the various propagators of the theory from the sole requirement of the complete gauge independence of $S$-matrix elements.



https://doi.org/10.1017/9781009402415.011 Published online by Cambridge University Press

## 10.1 General considerations

The application of the pinch technique in theories with tree-level symmetry breaking in general, and in the electroweak sector of the standard model in particular, is significantly more involved than in the QCD case. The reasons are both bookkeeping related, because of the proliferation of particles and Feynman diagrams, and conceptual, related to the correct allocation of the various pinch terms among the self-energies and vertices under construction:

1. There is a considerable increase in the number of sources of gauge-fixing parameter-dependent terms. In particular, in the $R_\xi$ gauges, the tree-level gauge-boson propagators – three massive gauge bosons ($W^\pm$ and $Z$) and a massless photon ($A$) – are given by

$$\Delta_i^{\mu\nu}(q) = \left[ g^{\mu\nu} - \frac{(1-\xi_i) q^\mu q^\nu}{q^2 - \xi_i M_i^2} \right] d_i(q^2)$$
$$d_i(q^2) = \frac{-\mathrm{i}}{q^2 - M_i^2}, \tag{10.1}$$

where $i = W, Z, A$ and $M_A^2 = 0$. In general, the gauge-fixing parameters $\xi_W$, $\xi_Z$, and $\xi_A$ will be considered different from one another. The inverse of the gauge-boson propagators, to be denoted by $\Delta^{-1}_{i,\mu\nu}$, is given by

$$\Delta^{-1}_{i,\mu\nu}(q) = \mathrm{i} \left[ (q^2 - M_i^2) g_{\mu\nu} - q_\mu q_\nu + \frac{1}{\xi_i} q_\mu q_\nu \right]. \tag{10.2}$$

Three unphysical (would-be) Goldstone bosons are associated with the three massive gauge bosons, to be denoted by $\phi^\pm$ and $\chi$. Their tree-level propagators are $\xi$ dependent, and given by

$$D_i(q) = \frac{\mathrm{i}}{q^2 - \xi_i M_i^2}, \tag{10.3}$$

with $i = W, Z$ (no Goldstone boson is associated with the photon). Note that

$$\Delta_i^{\mu\nu}(q) = U_i^{\mu\nu}(q) - \frac{q^\mu q^\nu}{M_i^2} D_i(q), \tag{10.4}$$

where

$$U_i^{\mu\nu}(q) = \left( g^{\mu\nu} - \frac{q^\mu q^\nu}{M_i^2} \right) d_i(q^2) \tag{10.5}$$

is the corresponding propagator in the so-called *unitary gauge* ($\xi_i \to \infty$). In addition, the ghost propagators are also given by $D_i(q)$, with $i = W, Z, A$

https://doi.org/10.1017/9781009402415.011 Published online by Cambridge University Press

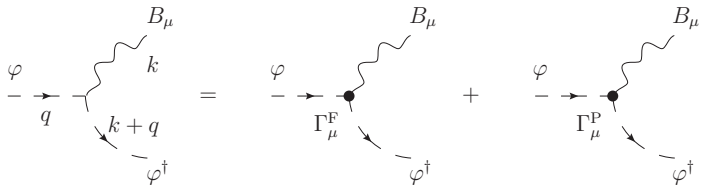


Figure 10.1. The PT decomposition of the generic elementary gauge-boson-scalar vertex $\Gamma_{B_\mu\varphi\varphi^\dagger}$.

(there is a massless ghost associated with the photon). Finally, the bare propagator of the physical Higgs boson is gauge-fixing parameter-independent at tree level, and given by $\Delta_H(q) = \mathrm{i}/(q^2 - M_H^2)$.

2. In addition to the longitudinal momenta coming from the propagators of the gauge bosons (proportional to $\lambda_i = 1 - \xi_i$) and the PT decomposition of the vertices involving three gauge bosons, a new source of pinching momenta appears, originating from graphs having an external (i.e., carrying the physical momentum $q$) would-be Goldstone boson. Specifically, interaction vertices, such as $\Gamma_{A_\alpha\phi^\pm\phi^\mp}$, $\Gamma_{Z_\alpha\phi^\pm\phi^\mp}$, $\Gamma_{W^\pm_\alpha\phi^\mp\chi}$, and $\Gamma_{W^\pm_\alpha\phi^\mp H}$, also furnish pinching momenta when the gauge boson is inside the loop carrying (virtual) momentum $k$. Such a vertex will then be decomposed as (see Figure 10.1)

$$\Gamma^{(0)}_\alpha(q,k,-q-k) = \Gamma^{\rm F}_\alpha(q,k,-q-k) + \Gamma^{\rm P}_\alpha(q,k,-q-k) \quad (10.6)$$

with

$$\begin{aligned}\Gamma^{(0)}_\alpha(q,k,-q-k) &= (2q+k)_\alpha \\ \Gamma^{\rm F}_\alpha(q,k,-q-k) &= 2q_\alpha \\ \Gamma^{\rm P}_\alpha(q,k,-q-k) &= k_\alpha, \end{aligned} \quad (10.7)$$

which is the scalar case analog of Eqs. (1.41), (1.42), and (1.43).

3. When the fermions involved (external or inside loops) are massive, the Ward identity of Eq. (1.45) receives additional contributions, which correspond precisely to the tree-level coupling of the would-be Goldstone bosons to the fermions. To see this concretely, let us consider the analog of the fundamental pinching Ward identity of Eq. (1.45), (e.g., in the case in which the incoming boson is a $W$). Contracting the $\Gamma_{W^+_\mu\bar{u}d}$ vertex with $k^\mu$ (the fermions $u$ and $d$ are isodoublet partners), we have

$$\not{k} P_L = P_R S_d^{-1}(k+p) - S_u^{-1}(p) P_L + [m_d P_R - m_u P_L], \quad (10.8)$$

where the chirality projection operators are defined according to $P_{L,R} = (1 \mp \gamma_5)/2$. The first two terms will pinch and vanish on shell, respectively,

https://doi.org/10.1017/9781009402415.011 Published online by Cambridge University Press

as they did in the case of QCD; the leftover term in the square bracket corresponds precisely to the coupling $\phi^+ \bar{u} d$ (the case involving the $\Gamma_{W_\mu^- \bar{d} u}$ is identical). A completely analogous Ward identity is obtained when the incoming boson is a $Z$. Again, contraction with the vertex $\Gamma_{Z \bar{f} f}$ furnishes a Ward identity similar to Eq. (10.8), with the additional term proportional to $m_f \gamma_5$, which corresponds to the coupling $\Gamma_{\chi \bar{f} f}$.

4. After the various pinch contributions have been identified, particular care is needed when allocating them among the PT quantities that one is constructing. So unlike the QCD case, in which all propagator-like pinch contributions were added to the only available self-energy, $\Pi_{\alpha\beta}$ (to construct $\widehat{\Pi}_{\alpha\beta}$), in the electroweak case, such pinch contributions must in general be split among various propagators. Thus, in the case of the charged channel, they will be shared in general between the self-energies $\Pi_{W_\alpha W_\beta}$, $\Pi_{W_\alpha \phi}$, $\Pi_{\phi W_\beta}$, and $\Pi_{\phi\phi}$. This is equivalent to saying that when forming the inverse of the $W$ propagator, in general, the longitudinal parts may no longer be discarded from the four-fermion amplitude because the external current is not conserved up to terms proportional to the fermion masses. The correct way of treating the longitudinal terms is to employ identities such as [3]

$$\begin{aligned} \mathrm{i} g_\alpha^\nu &= q^\nu q_\alpha D_i(q) - \Delta_i^{\nu\mu}(q) \left[ (q^2 - M_i^2) g_{\mu\alpha} - q_\mu q_\alpha \right] \\ \mathrm{i} q^\mu &= q^2 D_i(q) q^\mu + M_i^2 q_\nu \Delta_i^{\mu\nu}(q). \end{aligned} \tag{10.9}$$

The neutral channel is even more involved; one has to split the propagator-like pinch contributions among the self-energies $\Pi_{Z_\alpha Z_\beta}$, $\Pi_{A_\alpha A_\beta}$, $\Pi_{Z_\alpha A_\beta}$, $\Pi_{A_\alpha Z_\beta}$, $\Pi_{Z_\alpha \chi}$, $\Pi_{\chi Z_\beta}$, $\Pi_{\chi\chi}$, and $\Pi_{HH}$.

We emphasize that the preceding four points are tightly intertwined. The extra terms appearing in the Ward identity are precisely needed to cancel the gauge dependence of the corresponding graph in which the gauge boson is replaced by its associated Goldstone boson. In addition, as we will see in Section 10.3, when the external currents are not conserved, the appearance of the scalar-scalar or scalar-gauge-boson self-energies is crucial for enforcing the gauge-fixing parameter independence of the physical amplitude.

## 10.2 The case of massless fermions

We will now study the application of the pinch technique in the case where all fermions involved are massless. This simplification facilitates the PT procedure considerably because no scalar particles (Higgs and would-be Goldstone bosons) couple to the massless fermions. As a result, (1) the scalars can appear only

https://doi.org/10.1017/9781009402415.011 Published online by Cambridge University Press

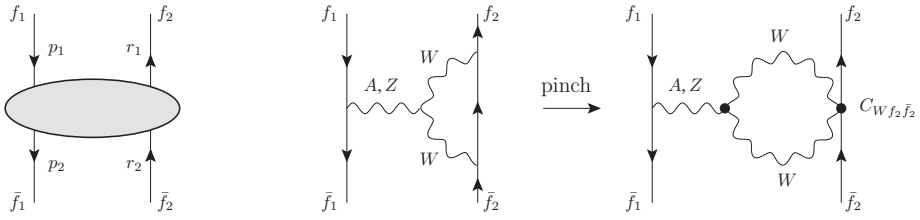


Figure 10.2. (*a*) The general process $f_1(p_1)\bar{f}_1(p_2) \to f_2(r_1)\bar{f}_2(r_2)$ mediated at tree level by a $Z$-boson and a photon and (*b*) the basic pinching and one of the unphysical vertices produced at the one-loop level.

*inside* the self-energy graphs, where they obviously cannot pinch; (2) Eq. (10.8) is practically reduced to its QCD equivalent; and (3) there are no self-energies with incoming scalars (i.e., no $\Pi_{W_\alpha\phi}$, $\Pi_{Z_\alpha\chi}$, $\Pi_{\phi\phi}$, etc.).

We now focus for concreteness on the the process $f_1(p_1)\bar{f}_1(p_2) \to f_2(r_1)\bar{f}_2(r_2)$, mediated at tree level by a $Z$-boson and a photon, as shown in Figure 10.2(*a*). At one-loop order, the box and vertex graphs furnish propagator-like contributions every time the Ward identity of Eq. (10.8) is triggered by a pinching momentum. Specifically, the term in Eq. (10.8) proportional to the inverse of the internal fermion propagator gives rise to a propagator-like term whose coupling to the external fermions $f$ and $\bar{f}$ (with $f = f_1, f_2$) is proportional to an effective vertex $C_{W_\alpha f\bar{f}}$ given by (see also Figure 10.2(*b*))

$$C_{W_\alpha f\bar{f}} = -\mathrm{i}\left(\frac{g_w}{2}\right)\gamma_\alpha P_L. \tag{10.10}$$

Note that this effective vertex is unphysical in the sense that it does not correspond to any of the elementary vertices appearing in the electroweak Lagrangian. However, it can be written as a linear combination of the two *physical* tree-level vertices $\Gamma_{A_\alpha f\bar{f}}$ and $\Gamma_{Z_\alpha f\bar{f}}$ given by

$$\begin{aligned}\Gamma_{A_\alpha f\bar{f}} &= -\mathrm{i}Q_f\gamma_\alpha \\ \Gamma_{Z_\alpha f\bar{f}} &= -\mathrm{i}[(s_w^2 Q_f - T_z^f)P_L + s_w^2 Q_f P_R],\end{aligned} \tag{10.11}$$

as follows:

$$C_{W_\alpha f\bar{f}} = \left(\frac{s_w}{2T_z^f}\right)\Gamma_{A_\alpha f\bar{f}} - \left(\frac{c_w}{2T_z^f}\right)\Gamma_{Z_\alpha f\bar{f}}. \tag{10.12}$$

In the preceding formulas, $Q_f$ is the electric charge of the fermion $f$ and $T_z^f$ is its $z$-component of the weak isospin. The identity established in Eq. (10.12) allows one to combine the propagator-like parts with the conventional self-energy graphs by writing $1 = d_i(q^2)d_i^{-1}(q^2)$.

https://doi.org/10.1017/9781009402415.011 Published online by Cambridge University Press

Next we will describe how the cancellation of the gauge-fixing parameter proceeds at the one-loop level for the simple case in which $f_1$ is a charged lepton, to be denoted by $\ell$, and $f_2$ is a neutrino, denoted by $\nu$. Of course, on the basis of general field-theoretic principles, one knows in advance that the entire amplitude will be gauge-fixing parameter independent. What is important to recognize, however, is that this cancellation goes through without having to carry out any of the integrations over virtual loop momenta, exactly as happened in the case of QCD. From the practical point of view, the extensive gauge cancellations that are implemented through the pinch technique finally amount to the statement that one may start out in the Feynman gauge, that is, set directly $\xi_w = 1$ and $\xi_z = 1$, with no loss of generality.

The cancellation of $\xi_z$ is easy to demonstrate. The box diagrams containing two $Z$-bosons (direct and crossed) form a $\xi_z$-independent subset. The way this works is completely analogous to the QED case, in which the two boxes contain photons: the $\xi_z$ dependence of the direct box cancels exactly against the gauge-fixing parameter dependence of the crossed one. The only other set of graphs with a $\xi_z$ dependence is the self-energy graphs; it is easy to show, by employing the simple algebraic identity

$$\frac{1}{k^2 - \xi_i M_i^2} = \frac{1}{k^2 - M_i^2} - \frac{(1-\xi_i)M_i^2}{(k^2 - M_i^2)(k^2 - \xi_i M_i^2)}, \tag{10.13}$$

that their sum is independent of $\xi_z$, separately for $ZZ$ and $AZ$.

Demonstrating the cancellation of $\xi_w$ is significantly more involved. In what follows, we set $\lambda_w \equiv 1 - \xi_w$ and suppress a factor $g_w^2 \int_k$. We also define

$$\begin{aligned} I_3 &\equiv \left\{(k^2 - \xi_w M_w^2)(k^2 - M_w^2)[(k+q)^2 - M_w^2]\right\}^{-1} \\ I_4 &\equiv \left\{(k^2 - \xi_w M_w^2)[(k+q)^2 - \xi_w M_w^2](k^2 - M_w^2)[(k+q)^2 - M_w^2]\right\}^{-1}. \end{aligned} \tag{10.14}$$

Note that terms proportional to $q_\alpha$ or $q_\beta$ may be dropped directly because the external currents are conserved (massless fermions).

To get a feel of how the pinch technique organizes the various gauge-dependent terms, consider the box graphs shown in Figure 10.3. We have

$$(a) = (a)_{\xi_w = 1} + \mathcal{V}_{W^\alpha \ell \bar{\ell}} \left(\lambda_w^2 I_4 k_\alpha k_\beta - 2\lambda_w I_3 g_{\alpha\beta}\right) \mathcal{V}_{W^\beta \nu \bar{\nu}}, \tag{10.15}$$

where the vertices $\mathcal{V}$ are defined according to

$$\begin{aligned} \mathcal{V}_{W_\alpha f \bar{f}} &= \bar{v}_f C_{W_\alpha f \bar{f}} u_f \\ \mathcal{V}_{V_\alpha f \bar{f}} &= \bar{v}_f \Gamma_{V_\alpha f \bar{f}} u_f; \qquad V = A,\ Z. \end{aligned} \tag{10.16}$$

The first term on the right-hand side (rhs) of Eq. (10.15) is the pure box, that is, the part that does not contain any propagator-like structures, whereas the second term

https://doi.org/10.1017/9781009402415.011 Published online by Cambridge University Press

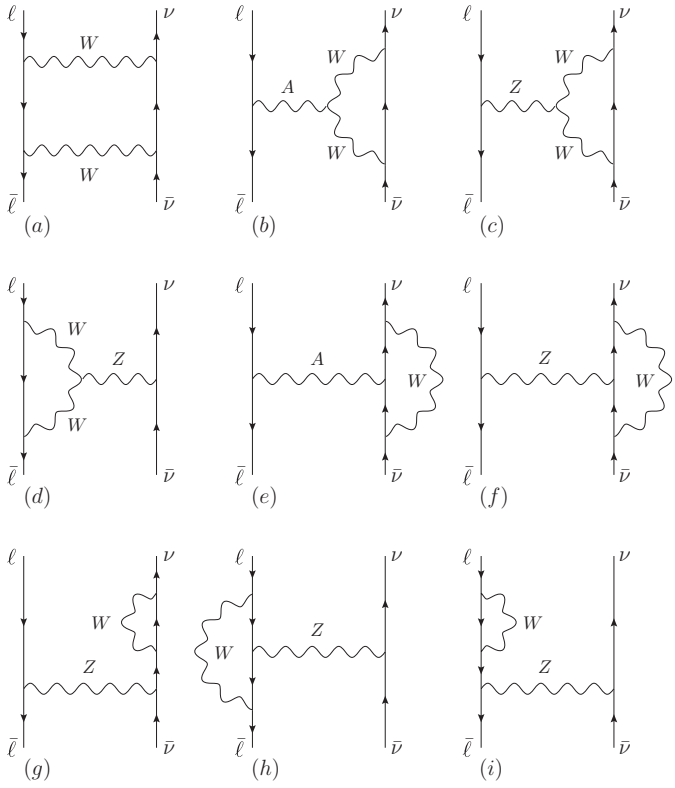


Figure 10.3. The box and vertex diagrams that depend on the gauge-fixing parameter $\xi_w$.

is the propagator-like contribution that must be combined with the conventional propagator graphs of Figure 10.4. To accomplish this, we employ Eq. (10.12) to write the unphysical vertices $\mathcal{V}_{W\ell\bar{\ell}}$ and $\mathcal{V}_{W\nu\bar{\nu}}$ in terms of the physical vertices, $\mathcal{V}_{A\ell\bar{\ell}}$, $\mathcal{V}_{Z\ell\bar{\ell}}$, and $\mathcal{V}_{Z\nu\bar{\nu}}$. Specifically, using that in our case $T_z^\ell = -1/2$ and $T_z^\nu = 1/2$, we have

$$\begin{aligned} C_{W^\alpha \ell\bar{\ell}} &= -s_w \Gamma_{A^\alpha \ell\bar{\ell}} + c_w \Gamma_{Z^\alpha \ell\bar{\ell}} \\ C_{W^\alpha \nu\bar{\nu}} &= -c_w \Gamma_{Z^\alpha \nu\bar{\nu}}. \end{aligned} \tag{10.17}$$

Equation (10.17) determines unambiguously the parts that must be appended to $\Pi_{Z_\alpha Z_\beta}$ and $\Pi_{A_\alpha Z_\beta}$ self-energies. To make this separation manifest, one must do the extra step of writing $d_z(q^2)d_z^{-1}(q^2) = d_A(q^2)d_A^{-1}(q^2) = 1$ to force the external tree-level propagators to appear explicitly (see Figure 10.5). Thus, from the propagator-like part of the box, we finally obtain

$$\begin{aligned} (a)_{A_\alpha Z_\beta} &= s_w c_w q^2 (q^2 - M_z^2) \left(\lambda_w^2 I_4 k_\alpha k_\beta - 2\lambda_w I_3 g_{\alpha\beta}\right) \\ (a)_{Z_\alpha Z_\beta} &= -c_w^2 (q^2 - M_z^2)^2 \left(\lambda_w^2 I_4 k_\alpha k_\beta - 2\lambda_w I_3 g_{\alpha\beta}\right). \end{aligned} \tag{10.18}$$

https://doi.org/10.1017/9781009402415.011 Published online by Cambridge University Press

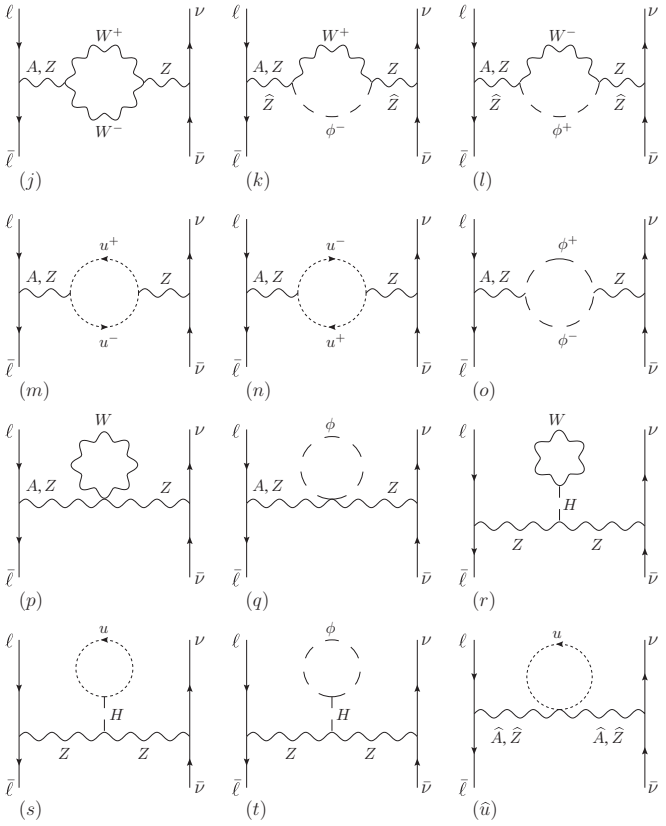


Figure 10.4. The $\xi_W$-dependent diagrams contributing to $\Pi_{Z_\alpha Z_\beta}$ and $\Pi_{Z_\alpha Z_\beta}$ and the corresponding diagrams in the BFM.

A similar procedure must be followed for the vertex graphs shown in Figure 10.3. Then all propagator-like terms identified from the boxes and the vertex graphs must be added to the conventional self-energy diagrams given in Figure 10.4. At this point, it would be a matter of straightforward algebra to verify that all $\xi_W$-dependent terms cancel; in doing that, Eq. (10.13) is useful. Of course, this cancellation proceeds completely independently for the $ZZ$ and $AZ$ contributions. Note that the inclusion of the tadpole graphs, namely, diagrams $(r)$, $(s)$, and $(t)$ of Figure 10.4, is crucial for the final cancellation of the gauge-fixing parameter-dependent contributions that do not depend on $q^2$. Exactly as happened in the QCD case, the gauge-fixing parameter cancellations amount effectively to choosing the Feynman gauge, $\xi_W = \xi_Z = 1$.

The next step is to consider the action of the remaining pinching momenta stemming from the three-gauge-boson vertices inside the non-Abelian diagrams $(b)$, $(c)$, and $(d)$ of Figure 10.3, exposed after employing the standard PT decomposition of Eqs. (1.41). The propagator-like contributions that will emerge from the action of

https://doi.org/10.1017/9781009402415.011 Published online by Cambridge University Press

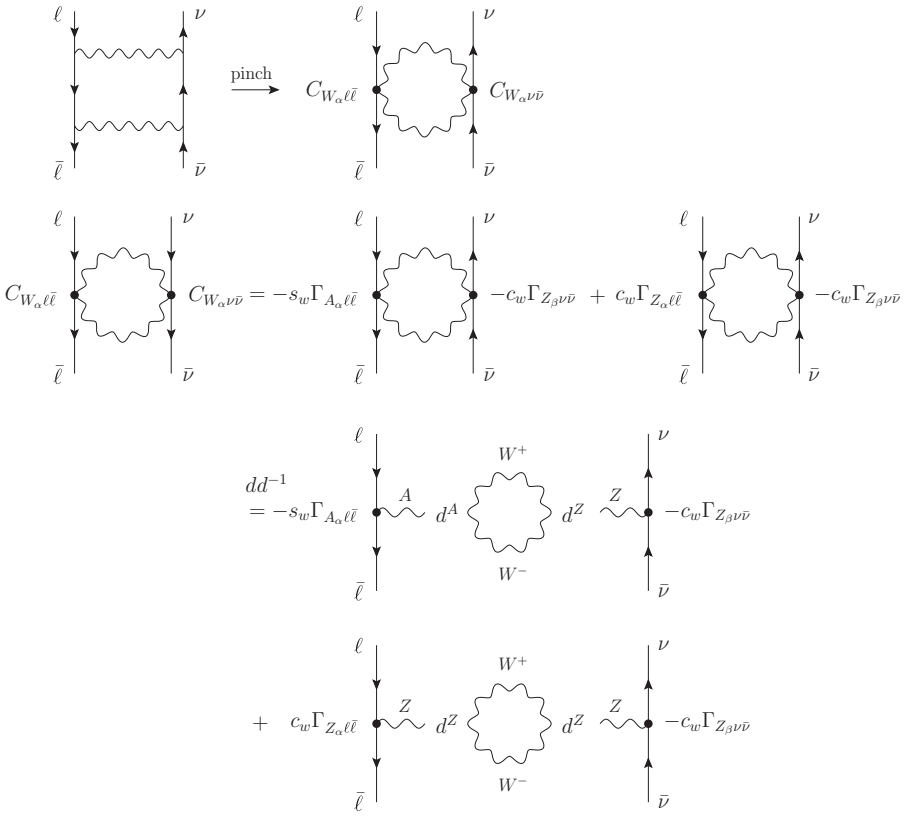


Figure 10.5. The procedure needed for splitting the propagator-like pieces coming from the $WW$ box among the different $AZ$ and $ZZ$ self-energies.

$\Gamma^{\rm P}$ must then be reassigned to the conventional self-energy graphs, thus giving rise to the one-loop PT self-energies, which in this case are $\widehat{\Pi}_{Z_\alpha Z_\beta}$ and $\widehat{\Pi}_{A_\alpha Z_\beta}$. The part of the vertex graph containing the $\Gamma^{\rm F}$, together with the Abelian graph which, in the Feynman gauge, remains unchanged, constitutes the one-loop PT vertices $A\nu\bar{\nu}$, $Z\nu\bar{\nu}$, and $Z\ell\bar{\ell}$, to be denoted by $\widehat{\Gamma}_{A\nu\bar{\nu}}$, $\widehat{\Gamma}_{Z\nu\bar{\nu}}$, and $\widehat{\Gamma}_{Z\ell\bar{\ell}}$, respectively.

The PT self-energies $\widehat{\Pi}_{Z_\alpha Z_\beta}$ and $\widehat{\Pi}_{Z_\alpha Z_\beta}$ are simply the sum of all propagator-like contributions, namely,

$$\begin{aligned}
\widehat{\Pi}_{Z_\alpha Z_\beta}(q) &= \Pi^{(\xi_W=1)}_{Z_\alpha Z_\beta}(q) + 4g_w^2 c_w^2 (q^2 - M_Z^2) g_{\alpha\beta} I_{WW}(q) \\
\widehat{\Pi}_{A_\alpha Z_\beta}(q) &= \Pi^{(\xi_W=1)}_{A_\alpha Z_\beta}(q) - 2g_w^2 s_w c_w (2q^2 - M_Z^2) g_{\alpha\beta} I_{WW}(q),
\end{aligned} \tag{10.19}$$

with

$$I_{WW}(q) = \int_k \frac{1}{(k^2 - M_w^2)[(k+q)^2 - M_w^2]}. \tag{10.20}$$

https://doi.org/10.1017/9781009402415.011 Published online by Cambridge University Press

It is relatively straightforward to prove that the $\xi_W$-independent PT self-energies given in Eqs. (10.19) coincide with their BFM counterparts computed at $\xi_W^Q = 1$. In particular, notice that (1) in the BFM, there is no $\widehat{A}W^{\pm}\phi^{\mp}$ interaction, and therefore graphs ($k$) and ($l$) of Figure 10.4 are absent in $\Pi_{\widehat{A}_\alpha \widehat{Z}_\beta}$, and (2) diagram ($\widehat{u}$) of the same figure, corresponding to the characteristic BFM four-field coupling $\widehat{V}\widehat{V}uu$, has been generated dynamically from the simple rearrangement of terms.

With a small extra effort, we can now obtain the closed expressions for $\widehat{\Pi}_{Z_\alpha Z_\beta}$ and $\widehat{\Pi}_{A_\alpha Z_\beta}$ in terms of the Passarino–Veltman functions [4]. We will only focus on the parts of the self-energies originating from Feynman graphs containing $W$ propagators, together with the associated Goldstone boson and ghosts. The contributions coming from the rest of the diagrams (e.g., containing loops with fermions or $Z$- and $H$-bosons) are common to the conventional and PT self-energies, i.e., $\Pi_{AZ}^{(\bar{f}f)} = \widehat{\Pi}_{AZ}^{(\bar{f}f)}$ and $\Pi_{ZZ}^{(\bar{f}f)} = \widehat{\Pi}_{ZZ}^{(\bar{f}f)}$, and we do not report them here. Therefore, the only Passarino–Veltman function that will appear is $B_0(q^2, M_W^2, M_W^2)$.

To that end, one may use the closed expressions for $\Pi_{Z_\alpha Z_\beta}^{(\xi_W=1)}$ and $\Pi_{A_\alpha Z_\beta}^{(\xi_W=1)}$ given by Denner [5] and add to them the pinch terms given in Eqs. (10.19) and (10.20). Using the identity $\mathrm{i}B_0(q^2, M_W^2, M_W^2) = 16\pi^2 I_{WW}(q)$, we finally obtain

$$
\begin{aligned}
\widehat{\Pi}_{AZ}^{(ww)}(q^2) = {} & \frac{\alpha}{4\pi}\frac{1}{3 s_w c_w} \\
& \times \left\{ \left[ \left( 21 c_w^2 + \frac{1}{2} \right) q^2 + (12 c_w^2 - 2) M_W^2 \right] B_0(q^2, M_W^2, M_W^2) \right. \\
& \left. - (12 c_w^2 - 2) M_W^2 B_0(0, M_W^2, M_W^2) + \frac{1}{3} q^2 \right\} \\
\widehat{\Pi}_{ZZ}^{(ww)}(q^2) = {} & -\frac{\alpha}{4\pi}\frac{1}{6 s_w^2 c_w^2} \\
& \times \left\{ \left[ \left( 42 c_w^4 + 2 c_w^2 - \frac{1}{2} \right) q^2 + (24 c_w^4 - 8 c_w^2 - 10) M_W^2 \right] \right. \\
& \times B_0(q^2, M_W^2, M_W^2) - (24 c_w^4 - 8 c_w^2 + 2) M_W^2 B_0(0, M_W^2, M_W^2) \\
& \left. + \frac{1}{3}(4 c_w^2 - 1)\, q^2 \right\}. \qquad (10.21)
\end{aligned}
$$

Note that $\widehat{\Pi}_{AZ}^{(ww)}(0) = 0$, exactly as happens for the corresponding subset of fermionic corrections: evidently, as a result of the PT rearrangement, bosonic and fermionic radiative corrections are treated on the same footing. This last property is important for phenomenonogical applications, as, for example, the unambiguous definition of the physical charge radius of the neutrinos (see Chapter 11).

https://doi.org/10.1017/9781009402415.011 Published online by Cambridge University Press

### 10.2.1 The unitary gauge

In the previous sections, we have applied the pinch technique in the framework of the linear renormalizable $R_\xi$ gauges, and we have obtained $\xi$-independent one-loop self-energies for the gauge bosons. What would happen, however, if one were to work *directly* in the unitary gauge? The unitary gauge is reached after gauging away the would-be Goldstone bosons through an appropriate field redefinition (which, at the same time, corresponds to a gauge transformation) $\phi(x) \to \phi'(x) = \phi(x)\exp(-i\zeta(x)/v)$, where $\zeta(x)$ denotes generically the Goldstone fields. Note that the unitary gauge is defined completely independently of the $R_\xi$ gauges; of course, operationally, it is identical to the $\xi_w, \xi_z \to \infty$ limit of the latter. In particular, in the unitary gauge, the $W$ and $Z$ propagators are given by Eq. (10.5), where $i = W, Z$. Given that the contributions of unphysical scalars and ghosts cancel in this gauge, the unitarity of the theory becomes *manifest* (hence its name). In the language employed before, *manifest unitarity* means that the optical theorem (a direct consequence of unitarity) holds in its strong version. The most immediate way to realize this is by noticing that the unitary gauge propagators Eq. (10.5) and the expression for the sum over the polarization vectors of a massive spin one vector boson (see Eq. (10.26)) are practically identical.

Since the early days of spontaneously broken non-Abelian gauge theories, the unitary gauge has been known to give rise to nonrenormalizable Green's functions in the sense that their divergent parts cannot be removed by the usual mass and field-renormalization counterterms. It is easy to deduce from the tree-level expressions of the gauge-boson propagators why this happens: the longitudinal contribution in Eq. (10.5) is divided by a squared mass instead of a squared momentum, i.e., $q^\mu q^\nu/M_i^2$ instead of $q^\mu q^\nu/q^2$, and therefore $U^i_{\mu\nu}(q) \sim 1$ as $q \to \infty$. As a consequence, when $U^i_{\mu\nu}(q)$ is inserted inside quantum loops (and $q$ is the virtual momentum that is being integrated over), it gives rise to highly divergent integrals. If dimensional regularization is applied, this hard short-distance behavior manifests itself in the occurrence of divergences proportional to high powers of $q^2$. Thus, at one loop, the divergent part of the $W$ or $Z$ self-energies proportional to $g_{\mu\nu}$ has the general form

$$\Pi^{\rm div}_{WW}(q^2) = \frac{1}{\epsilon}(c_1 q^6 + c_2 q^4 + c_3 q^2 + c_4)\,, \tag{10.22}$$

where the coefficients $c_i$, of appropriate dimensionality, depend on the gauge coupling and combinations of $M_w^2$ and $M_z^2$. The important point is that, whereas the last two terms on the rhs of Eq. (10.22) can be absorbed into mass and wave-function renormalization, as usual, the first two cannot be absorbed into

https://doi.org/10.1017/9781009402415.011 Published online by Cambridge University Press

a redefiniton of the parameters in the original Lagrangian because they are proportional to $q^6$ and $q^4$.

As was shown in a series of papers [6, 7, 8], when one puts together the individual Green's functions to form $S$-matrix elements, an extensive cancellation of all nonrenormalizable divergent terms takes place, and the resulting $S$-matrix element can be rendered finite through the usual mass and gauge coupling renormalization. Actually, in retrospect, this cancellation is nothing but another manifestation of the pinch technique (of course, the papers mentioned predate the pinch technique). Even though this situation may be considered acceptable from the practical point of view, in the sense that $S$-matrix elements may still be computed consistently, the inability to define renormalizable Green's functions has always been a theoretical shortcoming of the unitary gauge.

The actual demonstration of how to construct renormalizable Green's functions at one loop starting from the unitary gauge was given in [9]. The methodology is identical to that used in the context of the $R_\xi$ gauges: the propagator-like parts of vertices and boxes are identified and subsequently redistributed among the various gauge-boson self-energies. Evidently, the pinch contributions themselves contain divergent terms proportional to $q^6$ and $q^4$, which, when added to the analogous contributions contained in the conventional propagators, cancel exactly. After this cancellation, the remaining terms reorganize themselves in such a way as to give rise exactly to the *unique* PT gauge-boson self-energies, viz. Eqs. (10.21).

### *10.2.2 Absorptive construction in the electroweak sector*

We will now study with an explicit example how the PT subamplitudes of the electroweak theory satisfy the strong version of the optical theorem [10, 11]. As in the case of QCD, the fundamental reason for this may be traced back to a characteristic $s$-$t$ cancellation operating also in the presence of tree-level symmetry breaking.

Consider the process $f(p_1)\bar{f}(p_2)\to W^+(k_1)W^-(k_2)$, with $q = p_1 + p_2 = k_1 + k_2$ and $s = q^2 = (p_1 + p_2)^2 = (k_1 + k_2)^2 > 4M_W^2$. The corresponding tree-level amplitude, $\mathcal{T}^{\mu\nu}$, is given by two $s$-channel graphs, one mediated by a photon and the other by a $Z$-boson, to be denoted by $\mathcal{T}_A^{\mu\nu}$ and $\mathcal{T}_Z^{\mu\nu}$, respectively, and one $t$-channel graph, to be denoted by $\mathcal{T}_t^{\mu\nu}$, i.e. (see also Figure 10.6),

$$\mathcal{T}^{\mu\nu} = \mathcal{T}_{s,A}^{\mu\nu} + \mathcal{T}_{s,Z}^{\mu\nu} + \mathcal{T}_t^{\mu\nu}, \tag{10.23}$$

https://doi.org/10.1017/9781009402415.011 Published online by Cambridge University Press

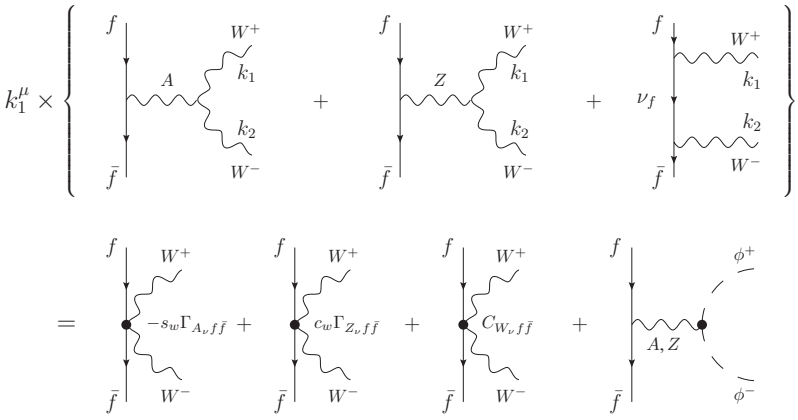


Figure 10.6. The fundamental $s$-$t$ cancellation for the process $f(p_1)\bar{f}(p_2) \to W^+(k_1)W^-(k_2)$.

where

$$\begin{aligned}
\mathcal{T}^{\mu\nu}_{s,A} &= -\mathcal{V}_{A^\alpha f\bar{f}} d_A(q^2) g_w s_w \Gamma^{\mu\nu}_\alpha(q, k_1, k_2), \\
\mathcal{T}^{\mu\nu}_{s,Z} &= \mathcal{V}_{Z^\alpha f\bar{f}} d_Z(q^2) g_w c_w \Gamma^{\mu\nu}_\alpha(q, k_1, k_2), \\
\mathcal{T}^{\mu\nu}_{t} &= -\frac{g_w^2}{2} \bar{v}_f(p_2)\gamma^\mu P_L \, S^{(0)}_{f'}(p_1 - k_1)\gamma^\nu P_L u_f(p_1).
\end{aligned} \tag{10.24}$$

Note that we have already used current conservation to eliminate the (gauge-fixing parameter-dependent) longitudinal parts of the tree-level photon and $Z$-boson propagators. Then,

$$\mathcal{M} = [\mathcal{T}_A + \mathcal{T}_Z + \mathcal{T}_t]^{\mu\nu} \, L_{\mu\mu'}(k_1) L_{\nu\nu'}(k_2) \left[\mathcal{T}^*_A + \mathcal{T}^*_Z + \mathcal{T}^*_t\right]^{\mu'\nu'}, \tag{10.25}$$

where the polarization tensor $L^{\mu\nu}(k)$ corresponds to a massive gauge boson, that is,

$$L_{\mu\nu}(k) = \sum_{\lambda=1}^{3} \varepsilon^\lambda_\mu(k)\varepsilon^\lambda_\nu(k) = -g_{\mu\nu} + \frac{k_\mu k_\nu}{M_W^2}. \tag{10.26}$$

On shell ($k^2 = M_W^2$), we have that $k^\mu L_{\mu\nu}(k) = 0$. Therefore, as in the QCD case, when the two non-Abelian vertices are decomposed as in Eq. (1.41), the $\Gamma^{\rm P}$ parts vanish, and only the $\Gamma^{\rm F}$ parts contribute in the $s$-channel graphs; we denote them by $\mathcal{T}^{\mu\nu}_{A,{\rm F}}$ and $\mathcal{T}^{\mu\nu}_{Z,{\rm F}}$, respectively.

Let us then study what happens when $\mathcal{T}_{\mu\nu}$ is contracted by a longitudinal momentum, $k_1^\mu$ or $k_2^\nu$, coming from the polarization tensors. Employing the appropriate

https://doi.org/10.1017/9781009402415.011 Published online by Cambridge University Press

tree-level Ward identities, we obtain

$$\begin{aligned} k_{1\mu}\mathcal{T}^{\mu\nu}_{A,\mathrm{F}} &= -s_w \mathcal{V}_{A^\nu f\bar{f}} + \mathcal{S}^\nu_A, \\ k_{1\mu}\mathcal{T}^{\mu\nu}_{Z,\mathrm{F}} &= c_w \mathcal{V}_{Z^\nu f\bar{f}} + \mathcal{S}^\nu_Z, \\ k_{1\mu}\mathcal{T}^{\mu\nu}_{t} &= \mathcal{V}_{W^\nu f\bar{f}}, \end{aligned} \tag{10.27}$$

with

$$\begin{aligned} \mathcal{S}^\nu_A &= -\mathcal{V}_{A^\alpha f\bar{f}} d_A(q^2) g_w s_w (k_1 - k_2)_\alpha k_2^\nu \\ \mathcal{S}^\nu_Z &= \mathcal{V}_{Z^\alpha f\bar{f}} d_Z(q^2) g_w c_w \left[(k_1 - k_2)_\alpha k_2^\nu - M_Z^2 g_{\alpha\nu}\right]. \end{aligned} \tag{10.28}$$

Adding by parts both sides of Eq. (10.27), we see that a major cancellation takes place: the pieces containing the vertices $\mathcal{V}_{A^\nu f\bar{f}}$ and $\mathcal{V}_{Z^\nu f\bar{f}}$ cancel against $\mathcal{V}_{W^\nu f\bar{f}}$ by virtue of Eq. (10.17), and one is left on the rhs with a purely $s$-channel contribution, namely,

$$k_{1\mu}\mathcal{T}^{\mu\nu} = \mathcal{S}^\nu_A + \mathcal{S}^\nu_Z. \tag{10.29}$$

An exactly analogous cancellation takes place when one contracts with $k_2^\nu$.

After the implementation of the preceding cancellations, we can isolate, e.g., the part of the squared amplitude that is purely $s$-channel–mediated by a $Z$-boson, to be denoted by $\widehat{\mathcal{M}}_{ZZ}$. It is composed of the sum of the following terms:

$$\widehat{\mathcal{M}}_{ZZ} = \mathcal{T}^{\mathrm{F}}_Z \cdot \mathcal{T}^{\mathrm{F}*}_Z - 2\frac{\mathcal{S}_Z \cdot \mathcal{S}^*_Z}{M_w^2} + \frac{(k_2 \cdot \mathcal{S}_Z)\cdot(k_2 \cdot \mathcal{S}^*_Z)}{M_w^4}. \tag{10.30}$$

After elementary algebra, we find

$$\widehat{\mathcal{M}}_{ZZ} = \mathcal{V}_{Z_\alpha f\bar{f}} d_Z(q^2) K^{\alpha\beta}_{ZZ} d_Z(q^2) \mathcal{V}_{Z_\beta f,\bar{f}}, \tag{10.31}$$

with

$$K^{\alpha\beta}_{ZZ} = -\frac{g_w^2}{c_w^2}\left[\left(8q^2c_w^4 - 2M_W^2\right) g^{\alpha\beta} + \left(3c_w^4 - c_w^2 + \frac{1}{4}\right)(k_1 - k_2)^\alpha (k_1 - k_2)^\beta\right]. \tag{10.32}$$

We must then integrate this last expression over the available phase space and isolate its coefficient proportional to $g^{\alpha\beta}$, to be denoted by $K_{ZZ}$. Then, if the optical theorem holds at the level of the $\widehat{\Pi}^{(WW)}_{ZZ}(q)$, we should have

$$2\Im m\,\widehat{\Pi}^{(WW)}_{ZZ}(q) = K_{ZZ}, \tag{10.33}$$

where the left-hand side (lhs) of Eq. (10.33) must be obtained from Eq. (10.21) by taking its imaginary part.

https://doi.org/10.1017/9781009402415.011 Published online by Cambridge University Press

Using for the lhs the elementary result

$$\Im m\, B_0(q^2, M_W^2, M_W^2) = 8\pi^2 \int_{\mathrm{PS}_{WW}}, \tag{10.34}$$

with $\int_{\mathrm{PS}_{WW}}$ the two $W$s phase space integral (see Section 1.7.2), and for the rhs that

$$\int_{\mathrm{PS}_{WW}} (k_1 - k_2)^\alpha (k_1 - k_2)^\beta = -\frac{1}{3}(q^2 - 4M_W^2) g^{\alpha\beta} \int_{\mathrm{PS}_{WW}}, \tag{10.35}$$

it is easy to verify that Eq. (10.33) is indeed satisfied.

At this point, one could go a step further and employ a twice-subtracted dispersion relation to reconstruct the real part of $\widehat{\Pi}_{ZZ}^{(WW)}(q)$. The end result of this procedure will coincide with the corresponding expression obtained from Eq. (10.21) after appropriate renormalization (for a detailed derivation, see [11]).

Finally, we return to the nonrenormalizability of the unitary gauges, now seen from the absorptive point of view. As mentioned in the previous subsection, in the unitary gauge, the strong version of the optical theorem is satisfied; in relation to this section, what this means is that the optical theorem is satisfied diagram by diagram, without having to resort explicitly to the $s$-$t$ cancellation. For example, the imaginary part of the conventional self-energy $\Pi_{ZZ}^{(WW)}(s)$ in the unitary gauge is given by

$$\Im m\, \Pi_{ZZ}^{(WW)}(s) \sim (s - M_Z)^2 \int_{\mathrm{PS}_{WW}} \mathcal{T}_Z^{\mu\nu} L_{\mu\mu'}(k_1) L_{\nu\nu'}(k_2) \mathcal{T}_Z^{*\mu'\nu'}. \tag{10.36}$$

What is the price one pays for *not* implementing explicitly the $s$-$t$ cancellation? Simply, the conventional subamplitudes, such as the one given earlier, contain terms that grow as $s^2$ or as $s^3$ (see, e.g., [11, 12]); indeed, the $s$-$t$ cancellation eliminates precisely terms of this type. Consequently, if one were to substitute the $\Im m\, \Pi_{ZZ}^{(WW)}(s)$ obtained from the rhs of Eq. (10.36) into a twice-subtracted dispersion relation – the maximum number of subtractions allowed by renormalizability – ultraviolet divergent real parts proportional to $q^4$ or $q^6$ would be encountered. Of course, these are precisely the nonrenormalizable terms encountered in Eq. (10.22), now obtained not from a direct one-loop calculation but rather from the combined use of unitarity and analyticity.

### *10.2.3 Background field method away from $\xi_Q = 1$: physical versus unphysical thresholds*

As mentioned already, the fact that the BFM Green's functions satisfy the same QED-like Ward identities for every value of the quantum gauge-fixing parameter $\xi_Q$ does not mean that the PT Green's functions, reproduced from the background

https://doi.org/10.1017/9781009402415.011 Published online by Cambridge University Press

field method at $\xi_Q = 1$, are simply some among an infinity of physically equivalent choices, parametrized by $\xi_Q$. This interpretation is not correct: the BFM Green's functions obtained away from $\xi_Q = 1$ are not physically equivalent to the privileged case of $\xi_Q = 1$. The following basic observation clarifies this point beyond any doubt: for $\xi_Q \neq 1$, the imaginary parts of the BFM electroweak self-energies include terms with unphysical thresholds [11, 10]. For example, for the one-loop contributions of the $W$ and its associated would-be Goldstone boson and ghost to $\tilde{\Pi}^{(WW)}_{ZZ}(\xi_Q, s)$, one obtains

$$\Im m\tilde{\Pi}^{(WW)}_{ZZ}(s,\xi_Q) = \Im m\widehat{\Pi}^{(WW)}_{ZZ}(s) + \frac{\alpha}{24 s_w^2 c_w^2}\left(\frac{s-M_Z^2}{sM_Z^4}\right) \times \left[W_1(s) + W_2(s,\xi_Q) + W_3(s,\xi_Q)\right], \tag{10.37}$$

with

$$\begin{aligned} W_1(s) &= f_1(s)\theta(s-4M_W^2) \\ W_2(s,\xi_Q) &= f_2(s,\xi_Q)\lambda^{1/2}(s,\xi_Q M_W^2,\xi_Q M_W^2)\theta(s-4\xi_Q M_W^2) \\ W_3(s,\xi_Q) &= f_3(s,\xi_Q)\lambda^{1/2}(s,M_W^2,\xi_Q M_W^2)\theta(s-M_W^2(1+\sqrt{\xi_Q})^2), \end{aligned} \tag{10.38}$$

where $\lambda(x,y,z) = (x-y-z)^2 - 4yz$ and

$$\begin{aligned} f_1(s) &= \left(8M_W^2+s\right)\left(M_Z^2+s\right) + 4M_W^2\left(4M_W^2+3M_Z^2+2s\right) \\ f_2(s,\xi_Q) &= f_1(s) - 4\left(\xi_Q-1\right)M_W^2\left(4M_W^2+M_Z^2+s\right) \\ f_3(s,\xi_Q) &= -2\left[8M_W^2+s-2\left(\xi_Q-1\right)M_W^2+\left(\xi_Q-1\right)^2\frac{M_W^4}{s}\right]\left(M_Z^2+s\right). \end{aligned} \tag{10.39}$$

These gauge-dependent unphysical thresholds (see the arguments of the $\theta$ functions) are artifacts of the BFM gauge-fixing procedure; in the calculation of any physical process, they cancel exactly against unphysical contributions from the imaginary parts of the one-loop vertices and boxes. After these cancellations have been implemented, one is left just with the contribution proportional to the tree-level cross section for the on-shell physical process $f\bar{f} \to W^+W^-$, with thresholds only at $q^2 = 4M_W^2$. In fact, by obtaining in the previous subsection the full $W$-related contribution to the PT self-energy, namely, $\widehat{\Pi}^{(ZZ)}_{WW}(s)$, directly from the on-shell physical process $f\bar{f} \to W^+W^-$, we have shown explicitly that in the background field method at $\xi_Q = 1$, the thresholds that occur at $q^2 = 4M_W^2$ are due solely to the physical $W^+W^-$ pair. We therefore conclude that the particular value $\xi_Q = 1$ in the background field method is distinguished on physical grounds from all other values of $\xi_Q$.

https://doi.org/10.1017/9781009402415.011 Published online by Cambridge University Press

### 10.3 Nonconserved currents and Ward identities

We now discuss some important issues related to the application of the pinch technique when the fermions are massive, as discussed in Section 2.2.5. Consider the elastic process $e^-(r_1)\nu_e(p_1) \to e^-(p_2)\nu_e(r_2)$, and concentrate on the charged channel, which, at tree level, is shown in Figure 10.7. The momentum transfer $q$ is defined as $q = p_1 - p_2 = r_2 - r_1$, and we will consider the electrons to be massive, with a mass $m_e$, whereas the neutrinos will be treated for simplicity as massless. The tree-level propagators of the $W$ and the corresponding Goldstone boson are those given in Eq. (10.1) and Eq. (10.3) (for $i = W$); the index $W$ will be suppressed in what follows. The elementary vertices describing the coupling of the charged bosons with the external fermions are $\Gamma_\alpha \equiv \Gamma_{W^+_\alpha \bar{\nu}_e e} = \Gamma_{W^-_\alpha \bar{e}\nu_e}$, $\Gamma_+ \equiv \Gamma_{\phi^+\bar{\nu}_e e}$, and $\Gamma_- \equiv \Gamma_{\phi^-\bar{e}\nu_e}$ and are given by

$$\Gamma_\alpha = \frac{\mathrm{i}g_w}{\sqrt{2}}\gamma_\alpha P_L; \qquad \Gamma_{+(-)} = -\frac{\mathrm{i}g_w}{\sqrt{2}}\frac{m_e}{M_W}P_{R(L)}. \tag{10.40}$$

When sandwiched between the external spinors, they are denoted by $\Gamma^\alpha_1 = \bar{u}_{\nu_e}(r_2)\,\Gamma^\alpha u_e(r_1)$, $\Gamma^\alpha_2 = \bar{u}_e(p_2)\,\Gamma^\alpha\, u_{\nu_e}(p_1)$, $\Gamma_1 = \bar{u}_{\nu_e}(r_2)\,\Gamma_+\, u_e(r_1)$, and $\Gamma_2 = \bar{u}_e(p_2)\,\Gamma_-\, u_{\nu_e}(p_1)$. The elementary identities

$$\begin{aligned} q_\alpha \Gamma^\alpha_{1,2} &= M_w \Gamma_{1,2} \\ \mathrm{i}\Gamma_{1,2} &= M_w q^\beta \Delta_{\beta\alpha}(q)\Gamma^\alpha_{1,2} + q^2 D(q)\Gamma_{1,2}, \end{aligned} \tag{10.41}$$

valid for every $\xi$, are also useful.

We will start by considering the $S$-matrix at tree level (Figure 10.7), to be denoted by $T_0$:

$$T_0 = \Gamma^\alpha_1\, \Delta_{\alpha\beta}(q)\, \Gamma^\beta_2 + \Gamma_1\, D(q)\, \Gamma_2\,. \tag{10.42}$$

Of course, $T_0$ must be $\xi$ independent, and it is easy to demonstrate that this is indeed so. Using Eqs. (10.4) and (10.41), it is elementary to verify that $T_0$ can be written as

$$T_0 = \Gamma^\alpha_1 U_{\alpha\beta}(q)\Gamma^\beta_2. \tag{10.43}$$

Thus, even though one works in the $R_\xi$ gauge, making no assumption on the value of $\xi$ (in particular, not taking the limit $\xi \to \infty$), one is led effectively to the unitary gauge, with no (unphysical) would-be Goldstone bosons present.

There is an alternative way of writing $T_0$ that makes manifest the role of the massless Goldstone bosons. It is well known that the Ward identities (or Slavnov–Taylor identities) in theories with spontaneous symmetry breaking maintain the same form as in the unbroken theory at the expense of introducing massless longitudinal poles. The role of these massless poles is obscured because, through the process of gauge

https://doi.org/10.1017/9781009402415.011 Published online by Cambridge University Press

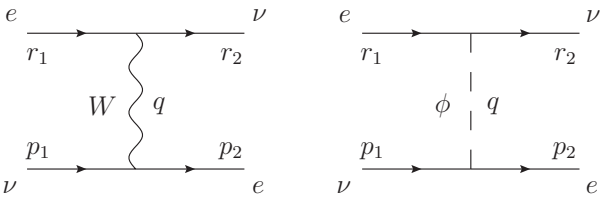


Figure 10.7. The process $e\nu_e \to e\nu_e$ at tree level in the standard model.

fixing, they can be changed to poles of arbitrary mass (as explained earlier). These massless poles do not appear in the $S$-matrix to the extent that they are absorbed by gauge bosons. However, simple algebra can recast the tree-level amplitude into a form in which the presence of the massless poles becomes manifest. Specifically, using the algebraic identity

$$\frac{1}{M^2} = \frac{1}{q^2} + \frac{q^2 - M^2}{q^2 M^2}, \tag{10.44}$$

we can write $U_{\alpha\beta}(q)$ as

$$U_{\alpha\beta}(q) = P_{\alpha\beta}(q) d_w(q^2) + \frac{q_\alpha q_\beta}{M_w^2} \frac{\mathrm{i}}{q^2}, \tag{10.45}$$

where we have used the transverse projector $P_{\alpha\beta}(q)$ defined in Eq. (1.26). Then Eq. (10.43) can be rewritten as

$$T_0 = \Gamma_1^\alpha P_{\alpha\beta}(q) d_w(q^2) \Gamma_2^\beta + \Gamma_1 \frac{\mathrm{i}}{q^2} \Gamma_2. \tag{10.46}$$

It turns out that the PT rearrangement of the physical amplitude allows the generalization of Eq. (10.43) and Eq. (10.46) to higher orders. To see how this happens, assume that the PT procedure has been carried out as usual (with the additional operational complications mentioned earlier), giving rise to the gauge-fixing parameter-independent self-energies $\Pi_{W_\alpha W_\beta}$, $\Pi_{W_\alpha \phi}$, $\Pi_{\phi W_\beta}$, and $\Pi_{\phi\phi}$, to be denoted by $\widehat{\Pi}_{\alpha\beta}$, $\widehat{\Theta}_\alpha$, $\widehat{\Theta}_\beta$, and $\widehat{\Omega}$, respectively (Figure 10.8). During this construction, it becomes clear that the cancellations of the gauge-fixing parameter-dependent loop contributions proceed without interfering with the the gauge-fixing parameter dependence of the tree-level propagators connecting the one-loop graphs to the external fermions. Of course, any residual gauge-fixing parameter dependence coming from these tree-level propagators (see Eqs. (10.1) and (10.3)) must also cancel to obtain fully gauge-fixing parameter-independent subamplitudes $\widehat{T}_1$ and $\widehat{T}_2$ ($\widehat{T}_3$, being boxlike, does not have external propagators and is already fully gauge-fixing parameter independent). It turns out that, quite remarkably, the requirement of this final gauge-fixing parameter cancellation imposes a set of nontrivial Ward identities on the one-loop PT self-energies and vertices [1, 3].

https://doi.org/10.1017/9781009402415.011 Published online by Cambridge University Press

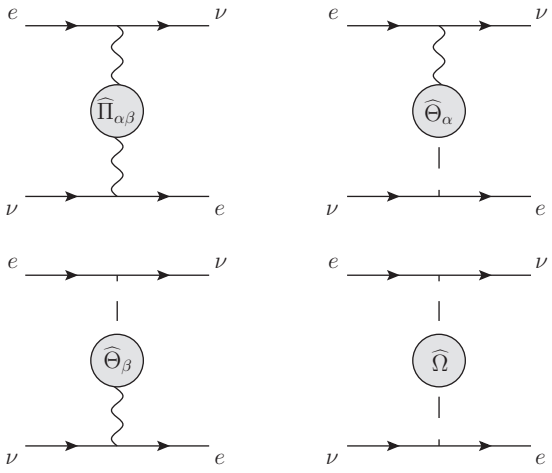


Figure 10.8. The $\xi$-independent PT self-energies (grey blobs); the tree-level propagators are still $\xi$-dependent. Requiring that any gauge-fixing parameter dependence coming from these tree-level propagators must cancel imposes a set of non-trivial Ward identities on the one-loop PT self-energies (and vertices).

We see how the Ward identities for the self-energies are derived from the requirement of the full gauge-fixing parameter independence of $\widehat{T}_1$. Neglecting tadpole contributions, we have that $\widehat{T}_1$ is given by

$$\begin{aligned}\widehat{T}_1 = {} & \Gamma_1^{\mu}\Delta_{\mu\alpha}(q)\widehat{\Pi}^{\alpha\beta}(q)\Delta_{\beta\nu}(q)\Gamma_2^{\nu} + \Gamma_1 D(q)\,\widehat{\Omega}(q)\,D(q)\Gamma_2 \\ & + \Gamma_1^{\mu}\Delta_{\mu\alpha}(q)\widehat{\Theta}^{\alpha}(q)D(q)\Gamma_2 + \Gamma_1 D(q)\widehat{\Theta}^{\beta}(q)\Delta_{\beta\nu}(q)\Gamma_2^{\nu}, \end{aligned} \tag{10.47}$$

or, after using Eq. (10.4),

$$\begin{aligned}\widehat{T}_1 = {} & \Gamma_1^{\mu}\left[U_{\mu\alpha}(q) - \frac{q_\mu q_\alpha}{M_w^2}D(q)\right]\widehat{\Pi}^{\alpha\beta}(q)\left[U_{\beta\nu}(q) - \frac{q_\beta q_\nu}{M_w^2}D(q)\right]\Gamma_2^{\nu} \\ & + \Gamma_1^{\mu}\left[U_{\mu\alpha}(q) - \frac{q_\mu q_\alpha}{M_w^2}D(q)\right]\widehat{\Theta}^{\alpha}(q)D(q)\Gamma_2 \\ & + \Gamma_1 D(q)\,\widehat{\Theta}^{\beta}(q)\left[U_{\beta\nu}(q) - \frac{q_\beta q_\nu}{M_w^2}D(q)\right]\Gamma_2^{\nu} + \Gamma_1 D(q)\widehat{\Omega}(q)D(q)\Gamma_2. \end{aligned} \tag{10.48}$$

This way of writing $\widehat{T}_1$ has the advantage of isolating all residual $\xi$ dependence inside the propagators $D(q)$. Demanding that $\widehat{T}_1$ be $\xi$ independent, we obtain as a condition for the cancellation of the quadratic terms in $D(q)$

$$q^{\beta}q^{\alpha}\widehat{\Pi}_{\alpha\beta}(q) - 2M_w q^{\alpha}\widehat{\Theta}_{\alpha}(q) + M_w^2\widehat{\Omega}(q) = 0, \tag{10.49}$$

https://doi.org/10.1017/9781009402415.011 Published online by Cambridge University Press

whereas for the cancellation of the linear terms, we must have

$$q^\alpha \widehat{\Pi}_{\alpha\beta}(q) - M_W \widehat{\Theta}_\beta(q) = 0. \tag{10.50}$$

From Eqs. (10.49) and (10.50), it follows that

$$q^\beta q^\alpha \widehat{\Pi}_{\alpha\beta}(q) = M_w^2 \widehat{\Omega}(q) \tag{10.51}$$

$$q^\alpha \widehat{\Theta}_\alpha(q) = M_w \widehat{\Omega}(q). \tag{10.52}$$

Equations (10.49) and (10.52) are the announced Ward identities. To be sure, they are identical to those obtained formally within the background field method but are derived through a procedure that has no apparent connection with the latter; indeed, all that one evokes is the full gauge-fixing parameter independence of the $S$-matrix. Applying an identical procedure for $\widehat{T}_2$, one obtains the corresponding Ward identity relating the higher-order PT vertices $\widehat{\Gamma}_\alpha$ and $\widehat{\Gamma}_\pm$.

Finally, the gauge-fixing parameter–independent $\widehat{T}_1$ is given by

$$\widehat{T}_1 = \Gamma_1^\mu U_{\mu\alpha}(q)\, \widehat{\Pi}^{\alpha\beta}(q) U_{\beta\nu}(q) \Gamma_2^\nu. \tag{10.53}$$

Notice that Eq. (10.53) is the higher-order generalization of Eq. (10.43).

We can now use the Ward identities derived previously to reformulate the $S$-matrix in a very particular way; specifically, we will show that the higher-order physical amplitude given earlier may be cast in the tree-level form of Eq. (10.46). Such a reformulation gives rise to a new transverse gauge-fixing parameter-independent $W$ self-energy $\widehat{\Pi}^{\mathrm{t}}_{\alpha\beta}$ with a gauge-fixing parameter-independent longitudinal part, exactly as in Eq. (10.46). Of course, the cost of such a reformulation is the appearance of massless Goldstone poles in our expressions. However, inasmuch as both the old and new quantities originate from the same unique $S$-matrix, all poles introduced by this reformulation will cancel against each other because the $S$-matrix contains no massless poles to begin with.

To see how this works out, write $\widehat{\Theta}_\alpha$ in the form

$$\widehat{\Theta}_\alpha(q) = q_\alpha \widehat{\Theta}(q)\,; \tag{10.54}$$

from Eq. (10.52), it follows that

$$\widehat{\Theta}(q) = \frac{M_w}{q^2} \widehat{\Omega}(q). \tag{10.55}$$

Then we can define $\widehat{\Pi}^{\mathrm{t}}_{\alpha\beta}(q)$ in terms of $\widehat{\Pi}^{\alpha\beta}(q)$ and $\widehat{\Theta}(q)$ as follows:

$$\widehat{\Pi}^{\mathrm{t}}_{\alpha\beta}(q) = \widehat{\Pi}_{\alpha\beta}(q) - \frac{q_\alpha q_\beta}{q^2} M_w \widehat{\Theta}(q). \tag{10.56}$$

https://doi.org/10.1017/9781009402415.011 Published online by Cambridge University Press

Evidently $\widehat{\Pi}^{\rm t}_{\alpha\beta}(q)$ is transverse, e.g., $q^\alpha \widehat{\Pi}^{\rm t}_{\alpha\beta}(q) = q^\beta \widehat{\Pi}^{\rm t}_{\alpha\beta}(q) = 0$. Moreover, using Eqs. (10.50) and (10.55),

$$\widehat{\Pi}^{\rm t}_{\alpha\beta}(q) = P_{\alpha\mu}(q)\widehat{\Pi}^{\mu\nu}(q)P_{\beta\nu}(q). \tag{10.57}$$

We may now reexpress $\widehat{T}_1$ of Eq. (10.53) in terms of $\widehat{\Pi}^{\rm t}_{\alpha\beta}$ and $\widehat{\Omega}$; using Eq. (10.45) and (10.41), we have

$$\widehat{T}_1 = \Gamma_1^\alpha d_w(q^2)\widehat{\Pi}^{\rm t}_{\alpha\beta}(q)d_w(q^2)\Gamma_2^\beta + \Gamma_1 \frac{\rm i}{q^2}\widehat{\Omega}(q)\frac{\rm i}{q^2}\Gamma_2. \tag{10.58}$$

Equation (10.58) is the generalization of Eq. (10.46): $\widehat{T}_1$ is the sum of two self-energies, one corresponding to a *transverse massive vector field* and one to a *massless Goldstone boson*. It is interesting to notice that the preceding rearrangements have removed the mixing terms $\widehat{\Theta}_\alpha$ and $\widehat{\Theta}_\beta$ between $W$ and $\phi$, thus leading to the generalization of the well-known tree-level property of the $R_\xi$ gauges to higher orders. It is important to emphasize again that the massless poles in the preceding expressions would not have appeared had we not insisted on the transversality of the $W$ self-energy (or the vertex); notice in particular that they are not related to any particular gauge choice, such as the Landau gauge ($\xi = 0$). A completely analogous procedure may be followed for the one-loop (and beyond) vertex [1], yielding the corresponding Abelian-like Ward identity; as in the case of the self-energy studied earlier, the Ward identity of the vertex is realized by means of massless Goldstone bosons.

## 10.4 The all-order construction

The all-order extension of the pinch technique in theories with spontaneous symmetry breaking can be achieved by resorting to the same algorithm described in Chapter 3 for QCD; however, now the construction is significantly more involved. First, depending on the nature of the line carrying the physical momentum $q$, there are four vertices to be constructed: two for the gauge-boson sector (charged ($W^\pm$) and neutral ($A$, $Z$)) and, as described in Section 10.1, two for the scalar sector (charged ($\phi^\pm$) and neutral ($\chi$, $H$)). In addition, the BRST symmetry, and therefore the Slavnov–Taylor identities, are now realized through Goldstone bosons; thus the different identities one needs to derive will have a richer structure than that shown in the QCD case (Eq. (3.5)). Finally, the comparison of the PT Green's functions with those of the background Feynman gauge is more laborious because of the proliferation of couplings, e.g., tri- and quadrilinear mixed gauge-boson–scalar vertices.

https://doi.org/10.1017/9781009402415.011 Published online by Cambridge University Press

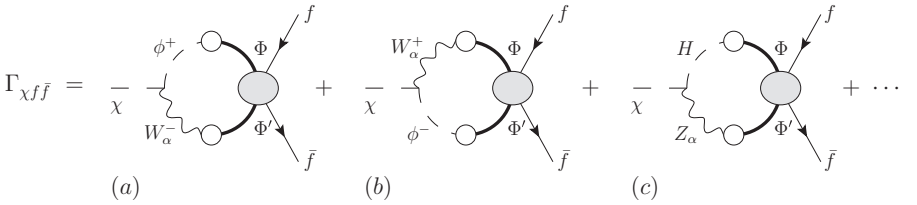


Figure 10.9. The subset of all the diagrams that contribute to the vertex $\Gamma_{\chi f\bar{f}}$ (in the $R_\xi$ gauge) and receive the action of pinching momenta. Here $\Phi$ and $\Phi'$ denote all fields allowed by the different couplings. The ellipses represent all remaining graphs, where pinching cannot take place. Finally, Bose-symmetric terms are not shown.

We illustrate some of the preceding points through a specific example, namely, the construction of the vertex $\widehat{\Gamma}_{\chi f\bar{f}}$. This case is particularly instructive because it exposes a new type of PT-driven cancellation not encountered so far in the book.

As usual, we choose the Feynman gauge as our starting point, thus receiving pinching momenta only from the tree-level vertices. Figure 10.9 shows all the graphs that must be contracted by the longitudinal momentum contained in the term $\Gamma^{\rm P}_\alpha(q,k_1,k_2)$. We will concentrate only on diagram $(a)$, which is proportional to a tree-level $\Gamma^{(0)}_{\chi\phi^+W^-_\alpha}$ vertex. Diagram $(b)$, proportional to $\Gamma^{(0)}_{\chi W^+_\alpha\phi^-}$, will give rise to very similar structures, whereas diagram $(c)$, proportional to $\Gamma^{(0)}_{\chi HZ_\alpha}$, does not mix with the previous two, and the corresponding analysis can be carried out separately.

The pinching part of diagram $(a)$ reads

$$(a)^{\rm P} = \frac{g_w}{2}\int k_2^\alpha \left[\mathcal{T}_{\phi^+W^-_\alpha}(k_1,k_2)\right]_{t,I}\,, \tag{10.59}$$

where $\mathcal{T}_{\phi^+W^-_\alpha}$ represents the amplitude $\phi^+W^-_\alpha \to f\bar{f}$, where the fermions are taken to be on shell. Then, similar to the QCD case, the pinching action amounts to the replacement

$$k_2^\alpha \left[\mathcal{T}_{\phi^+W^-_\alpha}\right]_{t,I} \;\to\; \left[k_2^\alpha \mathcal{T}_{\phi^+W^-_\alpha}\right]^{\rm PT}_{t,I} = \left[\mathcal{S}_{\phi^+W^-}\right]_{t,I}\,. \tag{10.60}$$

In this case, the (on-shell) Slavnov–Taylor identity gives [13]

$$\begin{aligned}
\mathcal{S}_{\phi^+W^-}(k_1,k_2) = {} & M_W D_c(k_1)D_c(k_2)\mathcal{G}_{\bar{c}^+c^-}(k_1,k_2)\\
& - M_W D_W(k_1)D_W(k_2)\mathcal{G}_{\phi^+\phi^-}(k_1,k_2)\\
& + \frac{g_w}{2}D_c(k_2)\left[{\rm i}\mathcal{Q}_{\{\chi c^+\}c^+}(k_1,k_2) + \mathcal{Q}_{\{Hc^+\}c^+}(k_1,k_2)\right]\\
& - g_w s_w D_c(k_2)\mathcal{Q}_{\{\phi^+c^A\}c^+}(k_1,k_2)\\
& + g_w\frac{c_w^2-s_w^2}{2c_w}D_c(k_2)\mathcal{Q}_{\{\phi^+c^Z\}c^+}(k_1,k_2),
\end{aligned} \tag{10.61}$$

https://doi.org/10.1017/9781009402415.011 Published online by Cambridge University Press

where $D_c$ is the propagator of the ghosts associated with the $W$-bosons. The functions $\mathcal{G}$ and $\mathcal{Q}$ are shown in Figure 3.4; their subindices denote the corresponding particle content, and curly brackets enclose fields evaluated at the same space-time point. Adding the preceding contribution (and the ones not explicitly considered here) to the remaining PT-inert diagrams furnishes the PT vertex $\widehat{\Gamma}_{\chi f \bar{f}}$.

One can next compare $\widehat{\Gamma}_{\chi f \bar{f}}$ with the background Feynman gauge vertex $\Gamma_{\widehat{\chi} f \bar{f}}$. First, it is fairly straightforward to show that the last three terms in Eq. (10.61) will generate the needed ghost-scalar quadrilinear couplings ($\widehat{\chi} H \bar{c}^- c^+$, $\widehat{\chi} \chi \bar{c}^- c^+$, $\widehat{\chi} \phi^+ \bar{c}^- c^A$, and $\widehat{\chi} \phi^+ \bar{c}^- c^Z$).

The remaining PT terms must be appropriately combined with some of the other $R_\xi$ diagrams contributing to $\Gamma_{\chi f \bar{f}}$. Consider first the trilinear scalar-ghost sector. In the $R_\xi$ gauge, it reads

$$-\frac{g_w}{2} M_W \int_{k_2} D_c(k_1) D_c(k_2) \, [\mathcal{G}_{\bar{c}^+ c^-}]_{t,I} \, , \tag{10.62}$$

and cancels precisely against the corresponding PT term (first term in Eq. (10.61)). This is the new type of PT cancellation mentioned earlier: within the PT, the absence of tree level coupling between a background field $\widehat{\chi}$ and two ghosts (see, e.g., Denner et al. [14]) is obtained dynamically. Similarly, had we chosen to construct the PT Higgs-fermion vertex $\widehat{\Gamma}_{H f \bar{f}}$ instead, these two terms would have added up, furnishing the correct background Higgs-ghost coupling.

Finally, consider the scalar-scalar trilinear sector. The second term in Eq. (10.61) gives a contribution to an effective PT vertex of the type $\chi \phi^+ \phi^-$. A similar contribution is generated from Figure 10.9($b$), whose pinching action is proportional to $[k_1^\alpha \mathcal{T}_{W_\alpha^+ \phi^-}(k_1, k_2)]_{t,I} = [\mathcal{S}_{W^+ \phi^-}]_{t,I}$. It turns out that these two contributions exactly cancel out in accordance with the absence of the (tree-level) couplings $\chi \phi^+ \phi^-$ and $\widehat{\chi} \phi^+ \phi^-$. Once again, when constructing the Higgs vertex $\widehat{\Gamma}_{H f \bar{f}}$, the two contributions would add up, thus providing the correct BFM coupling $\widehat{H} \phi^+ \phi^-$ when summed with the corresponding $R_\xi$ diagram. All remaining diagrams are identical to those of the background Feynman gauge because of the equality of the corresponding tree-level couplings. This concludes our (partial) proof of the equality $\widehat{\Gamma}_{\chi f \bar{f}} = \Gamma_{\widehat{\chi} f \bar{f}}$.

## References

[1] J. Papavassiliou, Gauge invariant proper self-energies and vertices in gauge theories with broken symmetry, *Phys. Rev.* **D41** (1990) 3179.
[2] G. Degrassi and A. Sirlin, Gauge invariant self-energies and vertex parts of the standard model in the pinch technique framework, *Phys. Rev.* **D46** (1992) 3104.

[3] J. Papavassiliou, Gauge independent transverse and longitudinal self-energies and vertices via the pinch technique, *Phys. Rev.* **D50** (1994) 5958.
[4] G. Passarino and M. J. G. Veltman, One loop corrections for $e^+ e^-$ annihilation into $\mu^+ \mu^-$ in the Weinberg model, *Nucl. Phys.* **B160** (1979) 151.
[5] A. Denner, Techniques for calculation of electroweak radiative corrections at the one-loop level and results for $W$ physics at LEP-200, *Fortschr. Phys.* **41** (1993) 307.
[6] S. Weinberg, Physical processes in a convergent theory of the weak and electromagnetic interactions, *Phys. Rev. Lett.* **27** (1971) 1688.
[7] S. Y. Lee, Finite higher-order weak and electromagnetic corrections to the strangeness-conserving hadronic beta decay in Weinberg's theory of weak interactions, *Phys. Rev.* **D6** (1972) 1803.
[8] T. Appelquist and H. R. Quinn, Divergence cancellations in a simplified weak interaction model, *Phys. Lett.* **B39** (1972) 229.
[9] J. Papavassiliou and A. Sirlin, Renormalizable $W$ self-energy in the unitary gauge via the pinch technique, *Phys. Rev.* **D50** (1994) 5951.
[10] J. Papavassiliou and A. Pilaftsis, Gauge-invariant resummation formalism for two point correlation functions, *Phys. Rev.* **D54** (1996) 5315.
[11] J. Papavassiliou, E. de Rafael, and N. J. Watson, Electroweak effective charges and their relation to physical cross sections, *Nucl. Phys.* **B503** (1997) 79.
[12] W. Alles, C. Boyer, and A. J. Buras, $W$ boson production in $e^+ e^-$ collisions in the Weinberg-Salam model, *Nucl. Phys.* **B119** (1977) 125.
[13] D. Binosi, Electroweak pinch technique to all orders, *J. Phys.* **G30** (2004) 1021.
[14] A. Denner, G. Weiglein, and S. Dittmaier, Application of the background field method to the electroweak standard model, *Nucl. Phys.* **B440** (1995) 95.